

Modeling Dinuclear Copper Sites of Biological Relevance: Synthesis, Molecular Structure, Magnetic Properties, and ^1H NMR Spectroscopy of a Nonsymmetric Dinuclear Copper(II) Complex. Microcalorimetric Determination of Stepwise Complexation of Copper(II) by a Nonsymmetric Dinucleating Ligand¹

Marcel Lubben,[†] Ronald Hage,[‡] Auke Meetsma,[†] Koos Býma,[†] and Ben L. Feringa*[†]

Department of Organic and Molecular Inorganic Chemistry, Groningen Center for Catalysis and Synthesis, University of Groningen, Nijenborgh 4, 9747 AG Groningen, The Netherlands, and Unilever Research Laboratories, Olivier van Noortlaan 120, 3133 AT Vlaardingen, The Netherlands

Received April 28, 1994[⊗]

The new nonsymmetric dinuclear copper(II) complex $[\text{Cu}_2\text{L}^1(\text{OAc})_2](\text{ClO}_4)$ (**7**) was synthesized by complexation of $\text{Cu}(\text{OAc})_2\cdot\text{H}_2\text{O}$ with a new nonsymmetric dinucleating ligand (**5**) which is formed *in situ* by condensation of 2-formyl-6-((4-methylpiperazin-1-yl)methyl)phenol (**3a**) with 2-(aminoethyl)pyridine. Complex **7** crystallizes in the monoclinic space group $P2_1/n$ with cell constants $a = 7.486(1)$ Å, $b = 22.472(2)$ Å, $c = 16.892(2)$ Å, $\beta = 102.75(1)^\circ$, $V = 2771.6(6)$ Å³, and $Z = 4$. The structure was determined at 130 K from 4890 out of a total of 7034 reflections with $R_F = 0.060$ and $R_{wF} = 0.060$. The crystal structure establishes the presence of a dinuclear copper core with distinct copper sites. One of the copper ions is coordinated by two sp^3 nitrogens whereas the other copper is coordinated by two sp^2 nitrogens. The two copper ions are bridged by a phenoxo group, by a syn-syn bidentate acetato bridge, and by a monodentate acetato bridge resulting in a Cu–Cu distance of 3.0293–(10) Å. The copper centers are weakly antiferromagnetically coupled with $2J = -15$ cm⁻¹. This weak antiferromagnetic coupling is reflected in the large isotropic shifts for the ligand protons in the ^1H NMR spectrum of **7**. 2D-COSY experiments and selective substitutions, leading to *p*-methyl-substituted complex **8**, were performed to allow assignments of the proton resonances. The complexation behavior of nonsymmetric ligand **5** is studied by microcalorimetric and UV–vis spectroscopic measurements. These techniques unambiguously establish the stepwise complexation behavior of the ligand; nonsymmetric dinuclear complex **7** is formed *via* the initial formation of a mononuclear copper complex. The enthalpy of formation of the first complexation step is -8.4 (± 0.2) kcal/mol ($K = 1.8$ (± 0.1) $\times 10^8$); for the second step a value of $\Delta H = -1.9$ (± 0.1) kcal/mol ($K = 1.1$ (± 0.1) $\times 10^5$) was obtained using microcalorimetry.

Introduction

In the last decade a large number of dinuclear copper complexes have been synthesized and structurally characterized in attempts to mimic the active sites of the type III dinuclear copper enzymes hemocyanin and tyrosinase.^{2,3} The interaction of these small-molecule active site analogues with dioxygen has been studied extensively in order to gain insight into reversible oxygen binding and oxygenase mechanisms of the type III dicopper enzymes. Both mononuclear^{4–7} and symmetrical dinuclear^{8,9} copper complexes have been used for this purpose. In particular the elegant biomimetic studies of Karlin,⁴ Kitajima,⁵ and co-workers have largely contributed to the understanding of the oxidized forms of hemocyanin, *i.e.* oxyhemocyanin,

whose structure was determined very recently by X-ray crystallography.¹⁰ First, tyrosinase was believed to contain an active site very similar to active site of hemocyanin¹¹ with two copper ions (CuA and CuB) coordinated by three histidines each. This was based upon the following spectroscopic similarities:¹² (a) both oxyhemocyanin and oxytyrosinase are EPR-silent, (b) the same UV–vis absorption bands with almost the same extinction coefficients are found for oxyhemocyanin and oxytyrosinase, and (c) identical spectral features are observed in the resonance Raman spectra of oxyhemocyanin and oxytyrosinase. However, there is substantial evidence now that, in the active site of tyrosinase, the two copper ions are coordinated by a different set of ligands. Comparison of the primary structures of hemocyanin and tyrosinase showed that only the ligands for

* Author to whom correspondence should be addressed.

[†] University of Groningen.

[‡] Unilever Research Laboratories.

[⊗] Abstract published in *Advance ACS Abstracts*, March 15, 1995.

- Presented in part at the 5th International Symposium on the Activation of Dioxygen and Homogeneous Catalytic Oxidation, College Station, TX, March 1993.
- For an excellent review, see: *Bioinorganic Chemistry of Copper*; Karlin, K. D., Tyeklár, Z., Eds.; Chapman and Hall: New York, 1993.
- Sorell, T. N. *Tetrahedron* **1989**, *45*, 3.
- Jacobson, R. R.; Tyeklár, Z.; Farooq, A.; Karlin, K. D.; Liu, S.; Zubieta, J. J. *Am. Chem. Soc.* **1988**, *110*, 3690.
- Kitajima, N.; Fujisawa, K.; Moro-oka, Y.; Toriumi, K. *J. Am. Chem. Soc.* **1989**, *111*, 8975.
- Maekawa, M.; Kitagawa, S.; Munakata, M.; Masuda, H. *Inorg. Chem.* **1989**, *28*, 1904.
- (a) Sorell, T. N.; Garrity, M. L. *Inorg. Chem.* **1991**, *30*, 210. (b) Thompson, J. S. *J. Am. Chem. Soc.* **1984**, *106*, 8308.
- (a) Karlin, K. D.; Hayes, J. C.; Gultneh, Y.; Cruse, R. W.; McKown, J. W.; Hutchinson, J. B.; Zubieta, J. *J. Am. Chem. Soc.* **1984**, *106*, 2121. (b) Gelling, O. J.; van Bolhuis, F.; Meetsma, A.; Feringa, B. L. *J. Chem. Soc., Chem. Commun.* **1988**, 552. (c) Casella, L.; Gullotti, M.; Pallanza, G.; Rigoni, L. *J. Am. Chem. Soc.* **1988**, *110*, 4221. (d) Réglér, M.; Jorand, C.; Waegell, B. *J. Chem. Soc., Chem. Commun.* **1990**, 1752. (e) Gelling, O. J.; Feringa, B. L. *J. Am. Chem. Soc.* **1990**, *112*, 7599. (f) Rockcliffe, D. A.; Martell, A. E. *Inorg. Chem.* **1993**, *32*, 3143.
- Feringa, B. L. In *Bioinorganic Chemistry of Copper*; Karlin, K. D., Tyeklár, Z., Eds.; Chapman and Hall: New York, 1993; p 306.
- Magnus, K. A.; Ton-That, H.; Carpenter, J. E. In *Bioinorganic Chemistry of Copper*; Karlin, K. D., Tyeklár, Z., Eds.; Chapman and Hall: New York, 1993; p 143.
- Gaykema, W. P. J.; Hol, W. G. J.; Vereijken, J. M.; Soeter, N. M.; Bak, H. J.; Beintema, J. *Nature* **1984**, *309*, 23.
- Himmelwright, R. S.; Eickman, N. C.; LuBien, C. D.; Lerch, K.; Solomon, E. I. *J. Am. Chem. Soc.* **1980**, *102*, 7339.

Table 1. Crystal Data and Data Collection, Structure Solution, and Refinement Parameters for $[\text{Cu}_2\text{L}^1(\text{OAc})_2](\text{ClO}_4)$ (7)

Crystal Data	
chem formula	$\text{C}_{24}\text{H}_{31}\text{ClCu}_2\text{N}_4\text{O}_9$
fw	682.08
crystal system	monoclinic
space group	$P2_1/n$, No. 14
a (Å)	7.486(1)
b (Å)	22.472(2)
c (Å)	16.892(2)
β (deg)	102.75(1)
V (Å ³)	2771.6(6)
Z	4
D_{calc} (g·cm ⁻³)	1.635
$F(000)$	1400
μ (Mo $K\alpha$) (cm ⁻¹)	16.9
approx crystal dimens (mm)	0.12 × 0.17 × 0.45
Data Collection	
radiation	Mo $K\alpha$ (λ 0.71073 Å)
monochromator	graphite crystal
temp (K)	130
θ range (deg)	1.24–27.0
no. of total data	7034
no. of unique data	6062
no. of obsd data	4890 ($I \geq 2.5\sigma(I)$)
Refinement	
no. of reflns	4890
no. of refined params	486
final agreement factors	
$R_F = \sum(F_o - F_c)/\sum F_o $	0.060
$R_{wF} = [\sum(w(F_o - F_c)^2)]^{1/2}$	0.060
$\sum w F_o ^2$	
goodness-of-fit ^a	3.625

^a Goodness of fit is defined as $S = [\sum w(|F_o| - |F_c|)^2/(m - n)]^{1/2}$ where m is the number of observed reflections and n is the number of parameters refined.

CuB are identical in both enzymes.¹³ For the ligands of CuA in tyrosinase, three possibilities are suggested by Lang and van Holde: (a) a histidine, (b) a cysteine or a methionine, or (c) no ligand at all. This means that the coordination sphere around the coppers is nonsymmetric with the copper nuclei either in a chemically or in a geometrically distinct environment. Additional proof is the observation that CuA is removed with less effort from the protein than CuB.^{13,14} Therefore the synthesis of dinucleating ligand systems with different affinities for both the copper ions is a great challenge as was already emphasized in a review by Sorell.³

Nevertheless, until now only a limited number of nonsymmetric dicopper complexes based on nonsymmetric dinucleating ligands are available.^{15,16} We present here the synthesis and the X-ray structure of a nonsymmetric dicopper(II) complex (7) which is based on a nonsymmetric dinucleating ligand (5) (Scheme 1). Details on the synthesis of this ligand and related nonsymmetric dinucleating ligands were published recently.¹⁷ Also the magnetic properties of nonsymmetric dicopper(II) complex 7 will be discussed together with its ¹H NMR spectral data. By making use of microcalorimetry and UV-vis spectroscopy, we will show that the nonsymmetric dinuclear complex is formed *via* initial formation of a mononuclear copper(II) complex.

(13) Lang, W. H.; Van Holde, K. E. *Proc. Natl. Acad. Sci. U.S.A.* **1991**, *88*, 244.

(14) Himmelwright, R. S.; Eickman, N. C.; Solomon, E. I. *Biochem. Biophys. Res. Commun.* **1978**, *81*, 243.

(15) Mahroof-Tahir, M.; Murthy, N. N.; Karlin, K. D.; Blackburn, N. J.; Shaikh, S. N.; Zubieta, J. *Inorg. Chem.* **1992**, *31*, 3001.

(16) Crane, J. D.; Fenton, D. E.; Latour, J. M.; Smith, A. J. *J. Chem. Soc., Dalton Trans.* **1991**, 2979.

(17) Lubben, M.; Feringa, B. L. *J. Org. Chem.* **1994**, *59*, 2227.

Table 2. Final Fractional Atomic Coordinates and Equivalent Isotropic Thermal Displacement Parameters for Non-H Atoms of the $[\text{Cu}_2\text{L}^1(\text{OAc})_2]^+$ Cation (Esd's in Parentheses)

	x	y	z	U_{eq} (Å ²) ^a
Cu1	0.17005(8)	0.08994(3)	0.22352(4)	0.0171(2)
Cu2	0.08206(8)	0.18723(3)	0.09675(4)	0.0159(2)
O1	0.0516(5)	0.17074(15)	0.20639(19)	0.0175(11)
O2	0.3139(5)	0.11563(16)	0.1451(2)	0.0201(11)
O3	0.5070(5)	0.13660(19)	0.2609(2)	0.0326(14)
O4	-0.0470(5)	0.04946(17)	0.1354(2)	0.0282(12)
O5	-0.1021(5)	0.12749(16)	0.0511(2)	0.0212(11)
N1	0.1367(6)	0.1916(2)	-0.0136(2)	0.0189(12)
N2	0.1732(5)	0.26763(19)	0.1266(2)	0.0174(12)
N3	0.0895(6)	0.07713(19)	0.3270(2)	0.0196(12)
N4	0.2853(6)	0.0119(2)	0.2701(2)	0.0219(12)
C1	0.1724(8)	0.1402(3)	-0.0477(3)	0.0241(17)
C2	0.1943(8)	0.1364(3)	-0.1268(3)	0.0254(19)
C3	0.1738(7)	0.1878(3)	-0.1730(3)	0.0278(19)
C4	0.1369(7)	0.2403(3)	-0.1389(3)	0.0250(19)
C5	0.1219(7)	0.2415(2)	-0.0584(3)	0.0205(16)
C6	0.0925(8)	0.2986(3)	-0.0169(3)	0.0237(17)
C7	0.2267(8)	0.3056(3)	0.0646(3)	0.0202(17)
C8	0.1830(7)	0.2913(3)	0.1969(4)	0.0215(18)
C9	0.1429(7)	0.2650(2)	0.2691(3)	0.0174(17)
C10	0.1743(7)	0.3004(2)	0.3393(3)	0.0230(17)
C11	0.1449(8)	0.2780(3)	0.4108(4)	0.0257(19)
C12	0.0819(7)	0.2204(3)	0.4134(3)	0.0234(17)
C13	0.0459(7)	0.1847(2)	0.3454(3)	0.0205(16)
C14	0.0803(6)	0.2060(2)	0.2719(3)	0.0174(16)
C15	-0.0317(8)	0.1231(3)	0.3489(3)	0.0223(17)
C16	0.2685(8)	0.0720(3)	0.3878(3)	0.0269(17)
C17	0.3895(8)	0.0290(3)	0.3523(3)	0.0247(17)
C18	0.0028(8)	0.0176(2)	0.3178(3)	0.0237(17)
C19	0.1261(9)	-0.0236(3)	0.2824(4)	0.0272(19)
C20	0.3996(10)	-0.0214(3)	0.2235(4)	0.030(2)
C21	0.4631(7)	0.1405(2)	0.1871(3)	0.0216(17)
C22	0.5734(9)	0.1756(4)	0.1397(5)	0.038(3)
C23	-0.1338(7)	0.0757(2)	0.0743(3)	0.0234(17)
C24	-0.3004(11)	0.0446(4)	0.0238(5)	0.047(3)

$$^a U_{\text{eq}} = \frac{1}{3} \sum_i U_{ij} a_i^* a_j^* a_i a_j$$

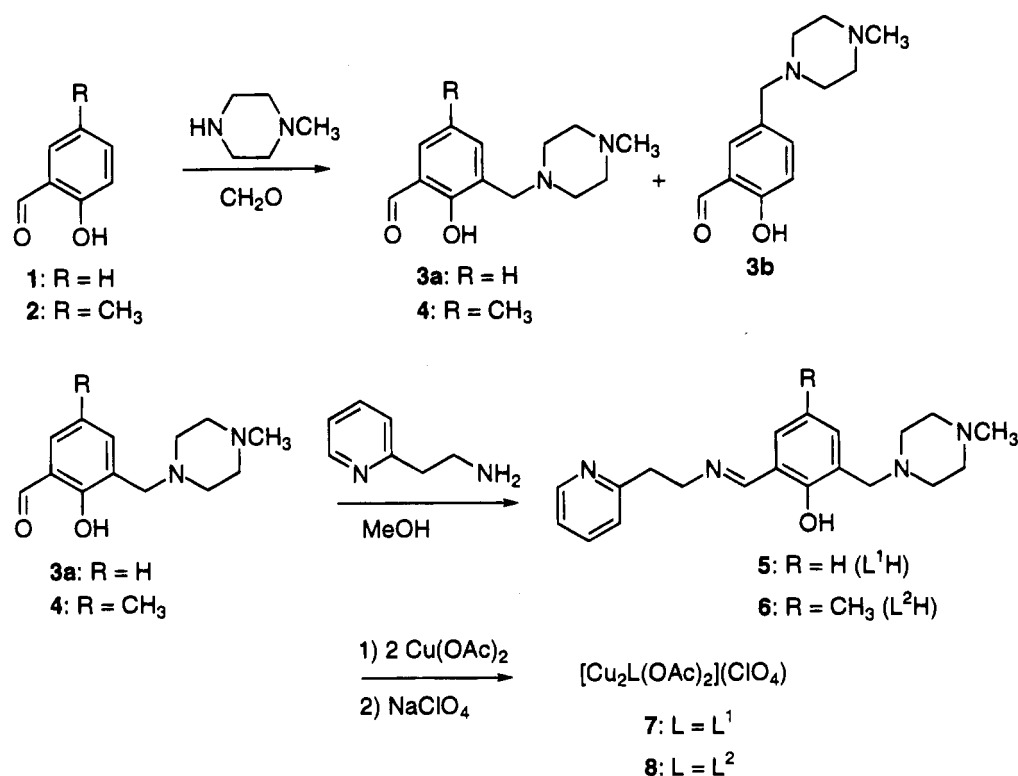
Table 3. Selected Bond Distances (Å) and Angles (deg) for the $[\text{Cu}_2\text{L}^1(\text{OAc})_2]^+$ Cation (Esd's in Parentheses)

Cu1—Cu2	3.0293(10)	Cu1—O1	2.013(4)
Cu1—O2	1.969(4)	Cu1—O4	2.148(4)
Cu1—N3	1.992(4)	Cu1—N4	2.035(4)
Cu2—O1	1.951(3)	Cu2—O2	2.375(4)
Cu2—O5	1.957(4)	Cu2—N1	1.997(4)
Cu2—N2	1.958(4)		
Cu2—Cu1—O1	39.41(9)	Cu2—Cu1—O2	51.59(11)
Cu2—Cu1—O4	78.62(10)	Cu2—Cu1—N3	131.60(13)
Cu2—Cu1—N4	154.55(11)	O1—Cu1—O2	85.86(15)
O1—Cu1—O4	92.32(14)	O1—Cu1—N3	92.72(16)
O1—Cu1—N4	165.62(14)	O2—Cu1—O4	95.76(14)
O2—Cu1—N3	161.66(16)	O2—Cu1—N4	105.35(16)
O4—Cu1—N3	102.57(16)	O4—Cu1—N4	95.41(16)
N3—Cu1—N4	73.78(17)	Cu1—Cu2—O1	40.94(10)
Cu1—Cu2—O2	40.51(9)	Cu1—Cu2—O5	78.92(10)
Cu1—Cu2—N1	129.64(13)	Cu1—Cu2—N2	118.36(11)
O1—Cu2—O2	76.97(14)	O1—Cu2—O5	91.38(15)
O1—Cu2—N1	170.54(17)	O1—Cu2—N2	92.17(14)
O2—Cu2—O5	93.93(14)	O2—Cu2—N1	93.99(15)
O2—Cu2—N2	110.48(14)	O5—Cu2—N1	86.42(16)
O5—Cu2—N2	155.50(16)	N1—Cu2—N2	93.64(16)
Cu1—O1—Cu2	99.65(15)		

Experimental Section

All reagents and solvents were reagent grade and used without further purification, unless indicated. 5-Methylsalicylaldehyde was prepared according to a literature procedure.¹⁸ Elemental analyses were performed in the Microanalytical Department of this laboratory. *Cau-*

(18) Casiraghi, G.; Casnati, G.; Puglia, G.; Sartori, G.; Terenghi, G. *J. Chem. Soc., Perkin Trans. I* **1980**, 1862.

Scheme 1. Two-Step Preparation of Nonsymmetric Ligands **5** and **6** and Subsequent Formation of Dinuclear Copper(II) Complexes **7** and **8**

tion: The perchlorate salts used in this study are all potentially explosive and should be handled with care.¹⁹

Synthesis of Ligands. 2-Formyl-6-((4-methylpiperazin-1-yl)methyl)phenol (**3a**) was prepared as follows: To 1-methylpiperazine (2.01 g, 20.1 mmol) was added (CH₂O)_n (0.60 g, 20.0 mmol). After the mixture was stirred for 1 h at 80 °C, salicylaldehyde **1** (2.45 g, 20.1 mmol) dissolved in methanol (10 mL) was added. The mixture was refluxed for 30 h. The methanol was evaporated to give an orange oil. Column chromatography on silica gel (CH₂Cl₂/MeOH, 9/1) afforded a fraction of pure **3a** (1.21 g, 26% yield), a fraction (0.664 g, 14% yield) consisting of a mixture of **3a** and **3b** (**3a/3b**, 7.1/1), and a fraction (0.56 g, 12% yield) consisting of a mixture of **3a** and **3b** (**3a/3b**, 1/3.4). All fractions were solids. Crystallization from hexane/ether gave pure **3a** as slightly yellow crystals: mp 86.0–87.0 °C; ¹H NMR (200 MHz) δ 2.28 (s, 3 H), 2.49–2.61 (br, 8 H), 3.70 (s, 2 H), 6.83 (dd, *J* = 7.7, 7.7 Hz, 1 H), 7.26 (m, 1 H), 7.60 (dd, *J* = 7.7, 1.7 Hz, 1 H), 10.30 (s, 1 H), 11.05 (br, 1 H); ¹³C NMR (50 MHz) δ 45.82 (q), 55.52 (t), 54.77 (t), 59.44 (t), 118.97 (d), 122.68 (s), 123.35 (s), 128.71 (d), 135.31 (d), 161.27 (s), 191.55 (d); HRMS *m/z* calcd for C₁₃H₁₈N₂O₂ 234.137, found 234.137. Anal. Calcd for C₁₃H₁₈N₂O₂: C, 66.64; H, 7.74; N, 11.96. Found: C, 66.35; H, 7.80; N, 11.70.

2-Formyl-4-methyl-6-((4-methylpiperazin-1-yl)methyl)phenol (**4**) was prepared as follows: To 1-methylpiperazine (1.478 g, 14.78 mmol) was added (CH₂O)_n (0.440 g, 14.66 mmol). After the mixture was stirred for 1 h at 80 °C, 5-methylsalicylaldehyde (**2**) (1.99 g, 14.63 mmol) dissolved in methanol (10 mL) was added. The mixture was refluxed for 20 h. The methanol was evaporated to give an orange oil. Column chromatography on silica gel (ethyl acetate/hexane, 1/1) followed by CH₂Cl₂/MeOH, 9/1, afforded **4** (2.701 g, 74% yield) as a yellow solid. Recrystallization from hexane/ether gave **4** as colorless crystals: mp 82.9–84.4 °C; ¹H NMR (200 MHz) δ 2.16 (s, 3 H), 2.21 (s, 3 H), 2.46 (br, 8 H), 3.59 (s, 2 H), 7.02 (d, 1 H, *J* = 1.7 Hz), 7.30 (d, 1 H, *J* = 1.7 Hz), 10.18 (s, 1 H), 10.25 (s, 1 H); ¹³C NMR (50 MHz) δ 20.15 (q), 45.73 (q), 52.43 (t), 54.68 (t), 59.28 (t), 122.24 (s), 123.16 (s), 128.08 (s), 128.30 (d), 136.39 (d), 159.08 (s), 191.52 (d); HRMS *m/z* calcd for C₁₄H₂₀N₂O₂ 248.152, found 248.153. Anal. Calcd

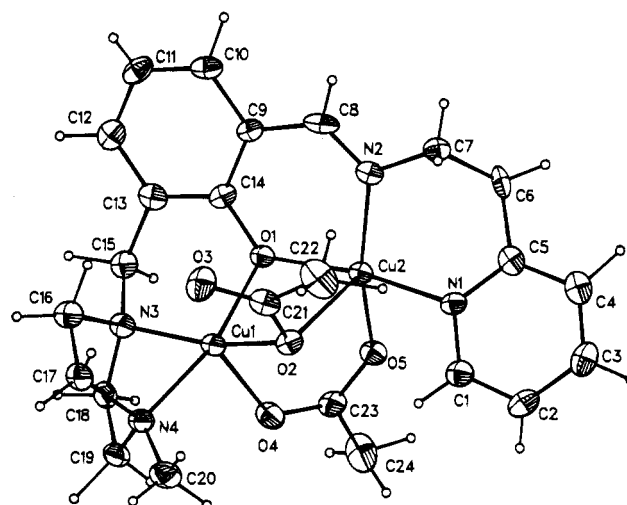


Figure 1. ORTEP plot of the [Cu₂L¹(OAc)₂]⁺ cation in complex **7**.

for C₁₄H₂₀N₂O₂: C, 67.72; H, 8.12; N, 11.28. Found: C, 67.32; H, 8.15; N, 11.15.

Synthesis of Complexes. [Cu₂L¹(OAc)₂](ClO₄) (**7**) was prepared as follows: To **3a** (0.236 g, 1.01 mmol) in MeOH (50 mL) was added 2-(aminoethyl)pyridine (0.123 g, 1.01 mmol). After 1 h of stirring at room temperature, Cu(OAc)₂·H₂O (0.40 g, 2.00 mmol) was added. After the mixture was refluxed for 1.5 h, NaClO₄·H₂O (0.200 g, 1.42 mmol) was added and the mixture was refluxed for another 0.5 h. The reaction mixture was filtered and the MeOH was removed *in vacuo*. A small amount of EtOH was added to the residue. The mixture was boiled for 5 min and filtered to afford pure **7** (0.43 g, 62% yield). Slow crystallization from CH₂Cl₂/EtOH afforded dark green crystals. Anal. Calcd for C₂₄H₃₁ClCu₂N₄O₉: C, 42.35; H, 4.59; Cu, 18.51; N, 8.24. Found: C, 41.52; H, 4.57; Cu, 18.83; N, 8.14.

[Cu₂L²(OAc)₂](ClO₄) (**8**) was prepared as follows: To **4** (91.1 mg, 0.367 mmol) in MeOH (3 mL) was added 2-(aminoethyl)pyridine (44.5 mg, 0.365 mmol). After 5 min of stirring at room temperature, Cu(OAc)₂·H₂O (146 mg, 0.731 mmol) was added. After 1 h of stirring at

(19) (a) Wolsey, W. C. *J. Chem. Educ.* **1973**, *50*, A335. (b) Raymond, K. N. *Chem. Eng. News* **1983**, *61* (Dec 5), 4.

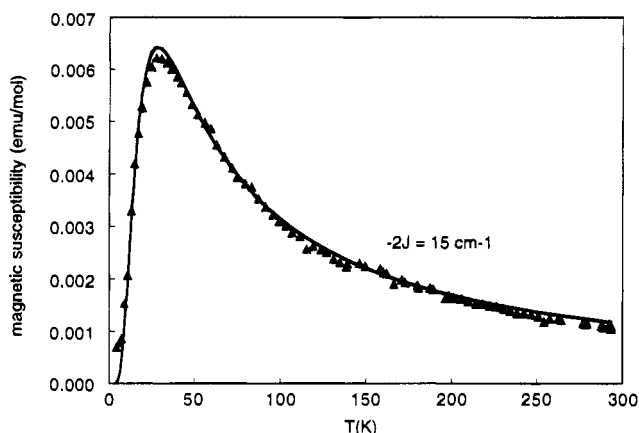


Figure 2. Temperature dependency of the molar susceptibility of **7**. Data (denoted as \blacktriangle) are plotted as molar susceptibility versus temperature. The solid line represents the calculated curve ($-2J = 15 \text{ cm}^{-1}$, $g = 2.0$).

room temperature, $\text{NaClO}_4 \cdot \text{H}_2\text{O}$ (82 mg, 0.586 mmol) was added and the mixture was stirred for another 5 min. After filtration, the methanolic solution was placed in an ethyl acetate bath. After 2 days of standing, **8** was isolated as dark green crystals (123 mg, 48% yield). Anal. Calcd for $\text{C}_{25}\text{H}_{33}\text{ClCu}_2\text{N}_4\text{O}_9$: C, 43.22; H, 4.79; Cu, 18.13; N, 8.07. Found: C, 42.82; H, 4.74; Cu, 17.98; N, 8.17.

Physical Measurements. ^1H NMR spectra were recorded on a Gemini-200 NMR spectrometer or on a Varian VXR-300 spectrometer. Chemical shifts are reported in δ units, relative to CD_3CN at $\delta = 1.93$ ppm.

UV-vis spectra were recorded on a Philips PU 8740 UV/vis spectrophotometer.

Microcalorimetric measurements were performed in an Omega titration calorimeter (Microcal, Northampton, MA). Experiments were performed at 35.2°C in a stirred reaction cell, installed in an omega titration microcalorimeter. Ligand and $\text{Cu}(\text{OAc})_2$ solutions were degassed before use. To 1.3249 mL of a 0.1 mM solution of nonsymmetric dinucleating ligand **5** in methanol was added a 2.0 mM solution of $\text{Cu}(\text{OAc})_2 \cdot \text{H}_2\text{O}$ in methanol in portions of $7 \mu\text{L}$ using a syringe. The heat absorbed or evolved was recorded, and after thermal equilibrium was reached, the next injection of $7 \mu\text{L}$ was executed. This procedure was repeated until the desired concentration range was covered. The solution was stirred to ensure complete mixing. Values for K of complexation were obtained through a nonlinear least-squares fit of the observed reaction heat for each step.²⁰

EPR spectra were obtained on a Bruker ECS 106 electron spin resonance spectrophotometer.

Magnetic measurements were performed in the temperature range 4–293 K with a fully automated DSM-8 susceptometer equipped with a TBT continuous-flow cryostat and a Drusch EAF 16 NC electromagnet, operating at *ca* 1.4 T. Data were corrected for magnetization of the sample holder and for diamagnetic contributions, which were estimated from the Pascal constants. Magnetic data were fitted to theoretical expressions by means of a simplex routine.²¹ All parameters (J , g , and p) were varied independently during the fitting procedure. This routine minimizes the function $R = |\sum(\text{obs} - \chi_{\text{calc}})^2 / \sum \chi_{\text{obs}}^2|^{1/2}$. No paramagnetic impurity was observed at very low temperature and was therefore not included in the fitting procedure.

X-ray Crystallography of $[\text{Cu}_2\text{L}^1(\text{OAc})_2](\text{ClO}_4)$ (7**).** A green, elongated parallelepiped-shaped crystal, cut along the long side, was used for characterization and data collection (approximate size $0.12 \times 0.17 \times 0.45$ mm). The crystal was mounted on top of a glass fiber and transferred into the cold nitrogen stream of the low-temperature unit²² mounted on an Enraf-Nonius CAD-4F diffractometer interfaced to a VAX-11/730 computer. Unit cell parameters and orientation matrix

were determined from a least-squares treatment of the SET4²³ setting angles of 22 reflections in the range $15.09 < \theta < 20.06^\circ$. The space group was derived from the observed extinct reflections. The unit cell was identified as monoclinic, space group $P2_1/n$. This choice was confirmed by the solution and refinement, although reduced cell calculations did indicate a centered orthorhombic metric lattice symmetry²⁴ (internal consistency of the data set was 57.4% in that case; in the monoclinic setting, 5.0%). Examination of the final atomic coordinates of the structure did not yield extra metric symmetry elements.²⁵ Crystal and/or instrumental instability was monitored by measurement of the intensities of three reference reflections that were collected after every 3 h of X-ray exposure time; there was no indication of crystal decomposition. A 360° ψ scan for a reflection close to axial (101) showed a variation in intensity of less than 8% about the mean value. Intensity data were corrected for Lorentz effects, polarization effects, and the scale variation but not for absorption. Standard deviations in the intensities based on counting statistics were increased according to an analysis of the excess variance²⁶ of the three reference reflections: $\sigma^2(I) = \sigma_{\text{CS}}^2(I) + (0.018I)^2$. Equivalent reflections were averaged, resulting in 4890 reflections satisfying the $I \geq 2.5\sigma(I)$ criterion of observability.

The structure was solved by Patterson methods, and extension of the model was accomplished by direct methods applied to difference structure factors using the program DIRDIF.²⁷ The positional and anisotropic thermal displacement parameters for the non-hydrogen atoms were refined with block-diagonal least-squares procedures (CRYLSQ)²⁸ minimizing the function $Q = \sum_h [w(|F_o| - k|F_c|)^2]$. A subsequent difference Fourier synthesis yielded positions for all the hydrogen atoms, whose coordinates and isotropic thermal displacement parameters were refined. The isotropic thermal displacement parameters for the hydrogen atoms H1, H7, and H18 converged to non-positive definite values. Weights were introduced in the final refinement cycles. The crystal exhibited some secondary extinction for which the F values were corrected by refinement of an empirical isotropic extinction parameter.²⁹ Final refinement on F_o by full-matrix least-squares techniques with anisotropic thermal displacement parameters for the non-hydrogen atoms and isotropic thermal displacement parameters for the hydrogen atoms converged at $R_F = 0.060$ ($R_{wF} = 0.060$). A final difference Fourier calculation revealed some residual electron density only in the vicinity of the heavy atoms (in the range -0.98 to $+1.99 \text{ e}/\text{\AA}^3$), which was of no chemical significance. Scattering factors were taken from Cromer and Mann.³⁰ Anomalous dispersion factors which were taken from Cromer and Liberman³¹ were included in F_c . All calculations were carried out on the CDC-Cyber 962-31 computer at the University of Groningen with the program packages XTAL³² and PLATON³³ (calculation of geometric data). Crystal data and experimental details of the structure determination are compiled in Table 1. The final fractional atomic coordinates and equivalent isotropic thermal displacement parameters for the non-hydrogen atoms are given in Table 2. Molecular geometry data are collected in Table 3.

Results and Discussion

Synthesis of Nonsymmetric Dinuclear Copper(II) Complexes **7** and **8**. Condensation of 2-formyl-6-((4-methylpiper-

(20) Weber, P. C.; Pantoliano, M. W.; Thompson, L. D. *Biochemistry* **1992**, *31*, 9350.

(21) Nelder, J. A.; Mead, R. *Comput. J.* **1965**, *7*, 308.

(22) van Bolhuis, F. J. *Appl. Crystallogr.* **1971**, *4*, 263.

(23) de Boer, J. L.; Duisenberg, A. J. M. *Acta Crystallogr.* **1984**, *A40*, C410.

(24) Spek, A. L. *J. Appl. Crystallogr.* **1988**, *21*, 578.

(25) (a) Le Page, Y. J. *Appl. Crystallogr.* **1987**, *20*, 264. (b) Le Page, Y. J. *Appl. Crystallogr.* **1988**, *21*, 983.

(26) McCandlish, L. E.; Stout, G. H.; Andrews, L. C. *Acta Crystallogr.* **1975**, *A31*, 245.

(27) The DIRDIF program system, Technical Report of the Crystallography Laboratory, University of Nijmegen, The Netherlands, 1992.

(28) Olthof-Hazekamp, R. In "CRYLSQ", XTAL3.0 Reference Manual; Hall, S. R., Stewart, J. M., Eds.; Universities of Western Australia and Maryland: Perth, Australia, and College Park, MD, 1990.

(29) Zachariasen, W. H. *Acta Crystallogr.* **1967**, *23*, 558.

(30) Cromer, D. T.; Mann, J. B. *Acta Crystallogr.* **1968**, *A24*, 321.

(31) Cromer, D. T.; Liberman, D. *J. Chem. Phys.* **1970**, *53*, 1891.

(32) XTAL3.0 Reference Manual; Hall, S. R., Stewart, J. M., Eds.; Universities of Western Australia and Maryland: Perth, Australia, and College Park, MD, 1990.

(33) Spek, A. L. *Acta Crystallogr.* **1990**, *A46*, C34.

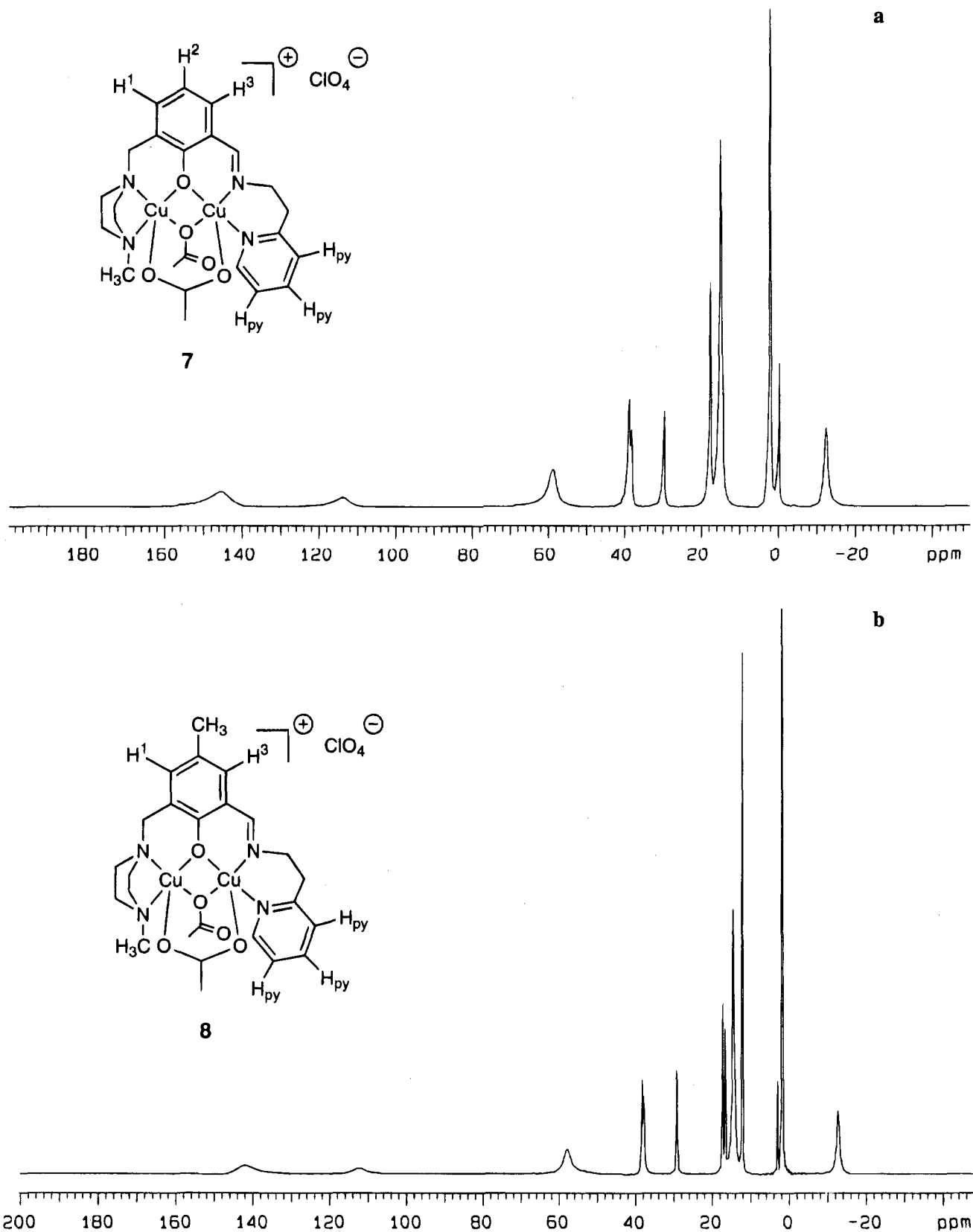


Figure 3. ^1H NMR spectra of **7** (a) and **8** (b) in CD_3CN .

azin-1-yl)methyl)phenol (**3a**) with 2-(aminoethyl)pyridine in methanol afforded imine **5** (Scheme 1), which is bright yellow. The imine was not isolated but *in situ* reacted with 2 equiv of $\text{Cu}(\text{OAc})_2 \cdot \text{H}_2\text{O}$ to afford a dinuclear copper(II) complex, which was crystallized as perchlorate salt **7**. Elemental analysis was in accordance with the stoichiometry $[\text{Cu}_2\text{L}^1(\text{OAc})_2]^+(\text{ClO}_4)$

where L^1 is the phenolate anion of **5**. The dicopper(II) complex $[\text{Cu}_2\text{L}^2(\text{OAc})_2](\text{ClO}_4)$ (**8**), where L^2 is the phenolate anion of **6**, was synthesized accordingly.

X-ray Structure of Nonsymmetric Dinuclear Complex 7. The molecular structure of the $[\text{Cu}_2\text{L}^1(\text{OAc})_2]^+$ cation is depicted in Figure 1.

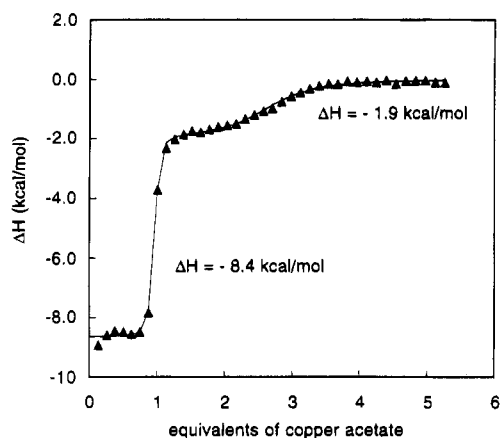


Figure 4. Microcalorimetric titration of nonsymmetric dinucleating ligand **5** with $\text{Cu}(\text{OAc})_2$ in methanol at 35.2 °C.

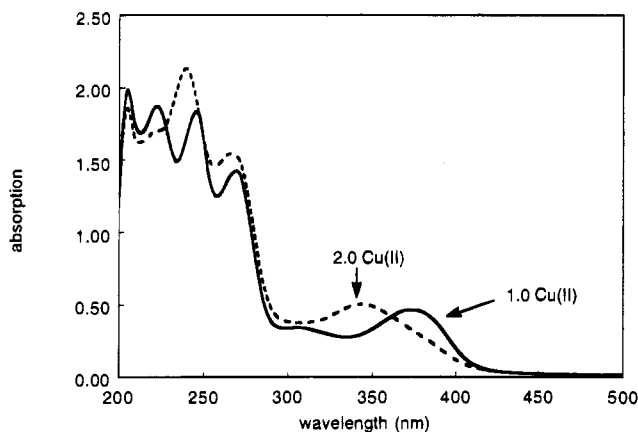


Figure 5. UV-vis titration of nonsymmetric dinucleating ligand **5** with $\text{Cu}(\text{OAc})_2$ in methanol at 25 °C.

The geometries around the copper nuclei are best described as square pyramidal with the apical positions being occupied by O4 for Cu1 and by O2 for Cu2.

The copper nuclei are bridged by a phenoxy oxygen in a relatively symmetric fashion resulting in comparable Cu1–O1 (2.013(4) Å) and Cu2–O1 (1.951(3) Å) bond distances. These bond lengths are in close agreement with those observed in other μ -phenoxy-bridged dicopper(II) complexes.^{8b,34,35}

The two copper nuclei are furthermore bridged by two acetate groups. One acetate group is syn-syn bidentate bridging, which is a very common bridging mode in dinuclear μ -carboxylato transition metal complexes especially in diiron and dimanganese complexes,³⁶ but this feature is also found in dicopper(II) complexes.^{16,34b} The Cu1–O4 distance of 2.148(4) Å differs markedly from the Cu2–O5 distance of 1.957(4) Å by 0.191 Å. This difference in bond length of the two metals to the oxygens of the syn-syn bidentate carboxylate bridge is usually not larger than 0.10 Å in diiron or dimanganese complexes. A difference of 0.19 Å is however found in a structurally related dicopper(II) complex with two syn-syn bidentate carboxylate bridges.^{34b}

The other acetate group in **7** is monodentate μ -oxo bridging. One oxygen (O2) of the acetate group is bridging between Cu1 and Cu2. The Cu2–O2 distance of 2.375(4) Å deviates from the Cu1–O2 distance of 1.969(4) Å by more than 0.4 Å. This is not unusual for monodentate carboxylate transition metal complexes.³⁷ Moreover there is a weak interaction between Cu1 and the other oxygen in the acetate group (O3), the so-called dangling oxygen. A Cu1–O3 distance of 2.675(4) Å is found.

Interestingly, in the symmetric analogue of **7**, *i.e.* a phenol-bridged dicopper(II) complex with two *N*-methylpiperazine arms, a symmetric bridging mode (syn-syn bidentate bridging) is observed for both the carboxylate residues.^{34c}

Both copper nuclei are coordinated by two nitrogen-containing groups each. These amine groups are however completely different in nature. Cu1 is coordinated by two sp^3 piperazine nitrogens (N3 and N4) whereas Cu2 is coordinated by two sp^2 nitrogens, one imine nitrogen (N2) and one pyridine nitrogen (N1). It should be noted that all the Cu–N distances fall in the range 1.96–2.04 Å. The N1–Cu2–N2 angle of 93.64–(16)° is markedly larger than the N3–Cu1–N4 angle of 73.78–(17)°.

The Cu1–Cu2 distance in the present complex is 3.0293–(10) Å, which is considerably shorter than the Cu–Cu distances of 3.297(3) Å^{34b} and 3.263(2) Å^{34c} in two related dicopper(II) complexes having one phenoxo and two syn-syn bidentate carboxylato bridges. It is also markedly shorter than the Cu–Cu distance of 3.392(1) Å found in a dicopper(II) complex with one monodentate μ -oxo carboxylate bridge and two syn-syn bidentate carboxylate bridges.³⁷ The Cu1–Cu2 distance in **7** is even shorter than the Cu–Cu distance of 3.257(2) Å in a dicopper(II) complex having two monodentate μ -oxo carboxylate bridges and one syn-syn bidentate carboxylate bridge.³⁷

Magnetic Measurements. Figure 2 shows the temperature dependency of the molar susceptibility of complex **7** between 293 and 4 K. The fitted susceptibility curve exhibits a maximum at $T = 27$ K. On the basis of the Bleany–Bowers equation, the singlet–triplet splitting, $2J$, is calculated to be -15 cm^{-1} . Thus a weak antiferromagnetic coupling is observed for the two copper(II) nuclei. This weak antiferromagnetic coupling can be explained as follows. The two copper(II) nuclei have a square pyramidal geometry with the apices occupied respectively by O4 for Cu1 and by O2 for Cu2. The magnetic orbital, *i.e.* the orbital containing the unpaired electron in a copper(II) nucleus in a square pyramidal geometry, is $d_{x^2-y^2}$. Since only the bridging phenolate oxygen (O1) is positioned in the equatorial plane of both Cu1 and Cu2, coupling can only occur through this bridging phenolate oxygen. In a series of structurally closely related dicopper(II) complexes, Murray *et al.* observed an increase in antiferromagnetic coupling as the Cu–O(phenolate)–Cu angle increases.^{34c} Karlin *et al.* also noted that the $-2J$ value should increase with increasing Cu–O(phenolate)–Cu angle.³⁸ Thus the small $-2J$ value found for nonsymmetric dicopper(II) complex **7** (-15 cm^{-1}) can be explained by the presence of a relatively small Cu1–O1–Cu2 angle of 99.65(15)°.³⁹ Despite the weak antiferromagnetic interaction observed using the magnetic susceptibility measurements and NMR spectroscopy (*vide infra*), no EPR spectrum

(34) (a) Sorell, T. N.; Jameson, D. L.; O'Connor, C. J. *Inorg. Chem.* **1984**, *23*, 190. (b) Nishida, Y.; Tokii, T.; Mori, Y. *J. Chem. Soc., Chem. Commun.* **1988**, 675. (c) Bertocello, K.; Fallon, G. D.; Hodgkin, J. H.; Murray, K. S. *Inorg. Chem.* **1988**, *27*, 4750.

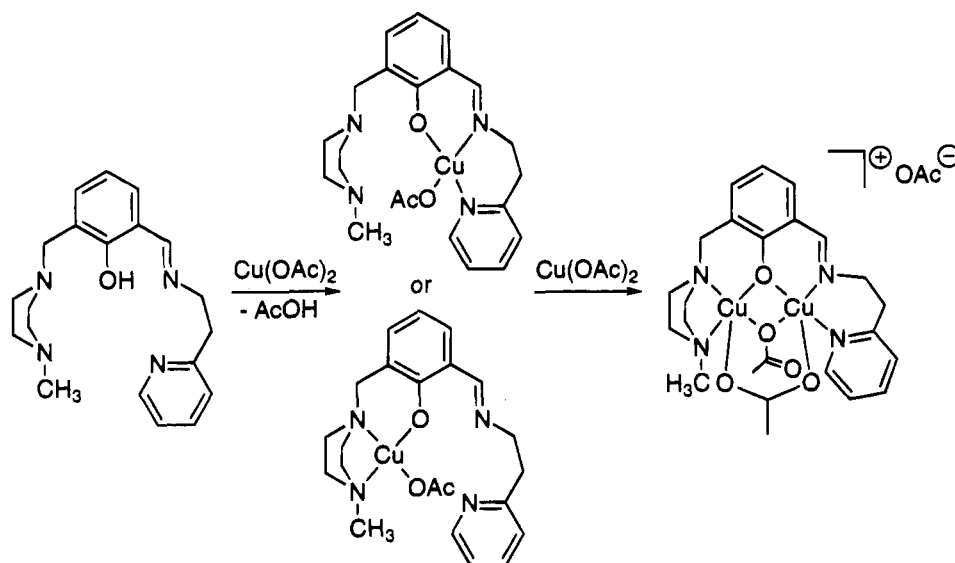
(35) Gelling, O. J.; Meetsma, A.; Feringa, B. L. *Inorg. Chem.* **1990**, *29*, 2816.

(36) (a) Armstrong, W. H.; Lippard, S. J. *J. Am. Chem. Soc.* **1983**, *105*, 4837. (b) Wieghardt, K.; Pohl, K.; Gebert, W. *Angew. Chem., Int. Ed. Engl.* **1983**, *22*, 727. (c) Borovik, A. S.; Hendrich, M. P.; Holman, T. R.; Münck, E.; Papaefthymiou, V.; Que, L., Jr. *J. Am. Chem. Soc.* **1990**, *112*, 6031. (d) Gulteh, Y.; Farooq, A.; Liu, S.; Karlin, K. D.; Zubieta, J. *Inorg. Chem.* **1992**, *31*, 3607.

(37) Rardin, R. L.; Tolman, W. B.; Lippard, S. J. *New. J. Chem.* **1991**, *15*, 417 and references cited therein.

(38) Karlin, K. D.; Farooq, A.; Hayes, J. C.; Cohen, B. I.; Rowe, T. M.; Sinn, E.; Zubieta, J. *Inorg. Chem.* **1987**, *26*, 1271.

(39) We acknowledge one reviewer who stated that the magnitude of the antiferromagnetic coupling depends not only on the Cu1–O1–Cu2 angle but also on the angle of the two XY planes in the dinuclear complex. The angle between the XY planes in complex **7** is 65.4(2)°. Strong antiferromagnetic coupling is only observed in dinuclear Cu(II) complexes in which the XY planes are coincident.

Scheme 2. Stepwise Complexation of $\text{Cu}(\text{OAc})_2$ by Nonsymmetric Dinucleating Ligand **5**

at room temperature or at 77 K both in acetonitrile solution and in the solid state has been observed.

^1H NMR Spectroscopy. The small value of the antiferromagnetic coupling between the copper(II) nuclei results in a ^1H NMR spectrum of **7** with large paramagnetic shifts (Figure 3a). The resonances are well resolved and cover a range of 180 ppm. NMR assignments are deduced from peak integrations, selective substitutions, 2D-COSY experiments, and comparison with NMR data for a structurally related phenolate-bridged dicopper(II) complex.⁶

The sharp peak at 0.1 ppm in the ^1H NMR spectrum of **7** disappears upon substitution of the para proton (H2) at the phenolate ring of **7** for a methyl group (para CH_3) as present in complex **8** (Figure 3b) and can consequently be assigned to the para proton (H2) of the phenolate ring. In the 2D-COSY spectrum of **7**, cross signals are observed for this para proton (H2) and the proton at 17.7 ppm as well as for H2 and the proton at 29.7 ppm. These resonances can thus be assigned to the meta protons (H1 and H3) at the phenolate ring in **7**. However, there is no coupling between H1 and H3 at the phenolate ring since no cross signals are observed. On the basis of integration of the peak at 17.7 ppm, it can be concluded that in addition to either H1 or H3 another proton shows a resonance at this value (17.7 ppm), resulting in overlap of the two peaks. This overlap is further proven by comparison with the ^1H NMR spectrum of the para-methyl-substituted complex **8** (Figure 3b), in which case these protons show separate resonances at 16.8 and 17.6 ppm. Furthermore, in the 2D-COSY spectrum of **7**, cross signals are observed for the proton resonance at 17.7 ppm and the proton resonances at 38.2 and 38.8 ppm. Moreover, cross peaks for the protons at 38.2 and 38.8 ppm are observed. As these three protons are all coupled, it can be concluded that these are the pyridine meta protons and the pyridine para proton (all denoted as Hpy). The broad resonance at 114 ppm is most likely the pyridine ortho proton on the basis of integration and significant line broadening because of its proximity to a paramagnetic copper(II) center. The only other possible assignment for this single proton is the imine proton. However, imine protons are usually obscured because of significant line broadening.⁶ The other broad resonances at 145, 59, and 15 ppm cannot be assigned with certainty, but they should originate from the various methylenic protons and/or from the bridging acetates. The 2D-COSY spectrum of **8**, the para-methyl-substituted analogue of **7**, is in agreement with the assignments

made for **7**. In the case of **8**, only cross signals are observed for all of the pyridine protons. The nonsymmetry of complexes **7** and **8** in solution is clearly demonstrated since the meta protons H1 and H3 of the phenolate unit show separate resonances as can be expected for a nonsymmetric complex.

Microcalorimetric Measurements. To study the complexation behavior of nonsymmetric dinucleating ligand **5** in solution, a 0.1 mM solution of ligand **5** in methanol was titrated with a 2.0 mM $\text{Cu}(\text{OAc})_2$ solution at 35.2 °C in a microcalorimeter cell. Figure 4 shows the absorbed or evolved heat per mole of added $\text{Cu}(\text{OAc})_2$. Two sequential S-shaped curves can be recognized from the figure. This observation corresponds to two discrete complexation steps which means that the nonsymmetric dinuclear complex is formed after the initial formation of a mononuclear copper(II) complex (Scheme 2). The difference in enthalpy between the horizontal parts of the S-shaped curve is the enthalpy of complexation. The first S-shaped curve shows the largest enthalpy change ($\Delta H = -8.4 (\pm 0.2)$ kcal/mol) presumably because of required deprotonation of the phenol group and the formation of the copper phenolate bond. The second enthalpy change is considerably smaller ($\Delta H = -1.9 (\pm 0.1)$ kcal/mol). The steep slope of the first S-shaped curve indicates a very tight binding mode for the first copper nucleus ($K = 1.8 (\pm 0.1) \times 10^8$) whereas the binding for the second copper nucleus is less tight ($K = 1.1 (\pm 0.1) \times 10^5$).

Although these measurements unambiguously show a stepwise complexation of $\text{Cu}(\text{OAc})_2$ by nonsymmetric dinucleating ligand **5**, it is not possible at this stage to differentiate between initial complexation at the pyridylimine or at the *N*-methylpiperazine moiety of **5** (Scheme 2). Experiments to isolate a mononuclear copper(II) complex based on ligand **5** have so far been unsuccessful.

UV-Vis Spectroscopy. A 0.1 mM solution of nonsymmetric dinucleating ligand **5** in methanol was titrated with a 2.0 mM $\text{Cu}(\text{OAc})_2$ solution at room temperature (Figure 5). After the addition of 1 equiv of $\text{Cu}(\text{OAc})_2$, the formation of an absorption maximum with $\lambda_{\text{max}} = 375$ nm ($\epsilon = 4700 \text{ M}^{-1} \text{ cm}^{-1}$) is observed. Addition of another equivalent of $\text{Cu}(\text{OAc})_2$ yields a spectral feature with $\lambda_{\text{max}} = 343$ nm ($\epsilon = 5100 \text{ M}^{-1} \text{ cm}^{-1}$). The latter λ_{max} and ϵ values are in good agreement with those of the nonsymmetric dicopper(II) complex $[\text{Cu}_2\text{L}^1(\text{OAc})_2](\text{ClO}_4)$, **7**, $\lambda_{\text{max}} = 344$ nm ($\epsilon = 4900 \text{ M}^{-1} \text{ cm}^{-1}$ in acetonitrile). The appearance of an absorption maximum at $\lambda_{\text{max}} = 375$ nm

($\epsilon = 4700 \text{ M}^{-1} \text{ cm}^{-1}$) after the addition of 1 equiv of $\text{Cu}(\text{OAc})_2$ clearly confirms the formation of a mononuclear species and rules out the possibility of a 1:1 mixture of dinuclear complex and free ligand.

Concluding Remarks. We have synthesized a new dinuclear copper complex which is one of the few structurally well-characterized nonsymmetric dicopper complexes. The nonsymmetric nature of the complex in the solid state is clearly established by its X-ray crystal structure. Despite of the observed weak antiferromagnetic coupling, resulting in large paramagnetic shifts for the ligand protons in the ^1H NMR spectrum of **7**, the majority of the resonances were sharp enough to perform 2D-COSY experiments allowing us to assign most of the proton resonances.

Microcalorimetric and UV-vis titration experiments of nonsymmetric dinucleating ligand **5** with $\text{Cu}(\text{OAc})_2 \cdot \text{H}_2\text{O}$ in methanol provides evidence for a stepwise complexation of the copper ions in the two binding sites of **5**. Although the magnetic properties of the oxidized forms of hemocyanin or tyrosinase are not accurately modeled by the present system, the different affinities observed for the two copper ions are consistent with

the different modes of binding of the two copper ions in tyrosinase.^{13,14}

Experiments to synthesize nonsymmetric complexes based on ligand **5** without the stabilizing carboxylate ligands are under current investigation. The reactivity of these complexes toward terminal oxidants might be relevant with respect to the functional modeling of tyrosinases. Karlin *et al.* already showed that the peroxide adduct of a nonsymmetric dicopper complex was more stable than that of the corresponding symmetric dicopper complex.¹⁵

Acknowledgment. We wish to thank J. Kolnaar for assistance with the magnetic measurements and Unilever, Vlaardingen, for financial support.

Supplementary Material Available: Tables giving crystal data, final fractional atomic coordinates, equivalent isotropic thermal displacement parameters, (an)isotropic thermal displacement parameters, bond distances, bond angles, and torsion angles (11 pages). Ordering information is given on any current masthead page.

IC940449R